

## Enhanced Arteriogenesis and Wound Repair in Dystrophin-Deficient *mdx* Mice

Stefania Straino, BS\*; Antonia Germani, PhD\*; Anna Di Carlo, PhD; Daniele Porcelli, MSc; Roberta De Mori, MSc; Antonella Mangoni, BS; Monica Napolitano, MD; Fabio Martelli, PhD; Paolo Biglioli, MD; Maurizio C. Capogrossi, MD

**Background**—The absence of functional dystrophin in Duchenne muscular dystrophy (DMD) patients and in *mdx* mice results in progressive muscle degeneration associated with necrosis, fibrosis, and inflammation. Because vascular supply plays a key role in tissue repair, we examined whether new blood vessel development was altered in *mdx* mice.

**Methods and Results**—In a model of hindlimb ischemia on femoral artery dissection, hindlimb perfusion, measured by laser Doppler imaging, was higher in *mdx* mice ( $0.67 \pm 0.26$ ) than in wild-type (WT) mice ( $0.33 \pm 0.18$ ,  $P < 0.03$ ). In keeping with these data, a significant increase in arteriole length density was found in *mdx* mice ( $13.6 \pm 8.4$  mm/mm<sup>3</sup>) compared with WT mice ( $7.8 \pm 4.6$  mm/mm<sup>3</sup>,  $P < 0.03$ ). Conversely, no difference was observed in capillary density between mice of the 2 genotypes. The enhanced regenerative response was not limited to ischemic skeletal muscle, because in a wound-healing assay, *mdx* mice showed an accelerated wound closure rate compared with WT mice. Moreover, a vascularization assay in Matrigel plugs containing basic fibroblast growth factor injected subcutaneously revealed an increased length density of arterioles in *mdx* ( $46.9 \pm 14.7$  mm/mm<sup>3</sup>) versus WT mice ( $19.5 \pm 5.8$  mm/mm<sup>3</sup>,  $P < 0.001$ ). Finally, serum derived from *mdx* mice sustained formation of endothelium-derived tubular structures in vitro more efficiently than WT serum.

**Conclusions**—These results demonstrate that arteriogenesis is enhanced in *mdx* mice both after ischemia and skin wounding and in response to growth factors. (*Circulation*. 2004;110:3341-3348.)

**Key Words:** muscles ■ genetics ■ vessels

Muscular dystrophies are a group of genetic diseases characterized by progressive degenerative changes in skeletal and cardiac muscle.<sup>1</sup> The most common muscular dystrophies involve mutations of the dystrophin-glycoprotein (DGC) complex, which is constituted of the intracellular proteins dystrophin and syntrophin and the sarcolemmal proteins dystroglycan ( $\alpha$  and  $\beta$  subunits) and sarcoglycans ( $\alpha$ ,  $\beta$ ,  $\gamma$ , and  $\delta$  subunits).<sup>2</sup> The oligomeric complex spans the sarcolemma and links intracellular actin cytoskeleton to the extracellular matrix. DGC complexes are also present in a variety of nonmuscle cells.<sup>3</sup> Dystrophin mutations are the most common cause of muscular dystrophy, accounting for both the Duchenne (DMD) and Becker phenotypes.<sup>4</sup> The *mdx* mouse is a murine model of muscular dystrophy in which a non-sense mutation in the dystrophin gene abrogates dystrophin expression.<sup>5</sup> Although the primary defect in dystrophic muscle is very well characterized, the relationship between the absence of the protein dystrophin and the pathogenetic mechanisms of DMD is still unclear.

### See p 3290

The lack of functional dystrophin protein destabilizes the DGC complex and alters signal transduction pathways, thereby rendering muscle fibers susceptible to damage.<sup>1</sup> Recent evidence suggests that numerous factors could be involved in the pathogenesis of muscular dystrophies.

Growth factors, cytokines, and chemokines represent essential elements in the modulation of muscle cell regeneration and differentiation. Interestingly, many growth factors and chemokines, such as basic fibroblast growth factor (bFGF),<sup>6</sup> monocyte chemoattractant protein-1 (MCP-1),<sup>7,8</sup> and nerve growth factor,<sup>9</sup> are upregulated in *mdx* mice. However, their role in DMD pathogenesis is still unclear. Moreover, disruption of muscle membrane repair machinery results in progressive muscular dystrophy in the presence of a functional DGC complex.<sup>10</sup>

Dystrophin protein is expressed not only in skeletal muscle cells but also in vascular smooth muscle and endothelial

Received April 16, 2004; revision received September 9, 2004; accepted September 24, 2004.

From the Laboratorio di Biologia Vascolare e Terapia Genica, Centro Cardiologico I, Monzino, IRCCS, Milan (S.S., A.G., A.D.C., A.M., P.B.), and the Laboratorio di Patologia Vascolare, Istituto Dermopatico dell'Immacolata, IRCCS, Rome (D.P., R.D.M., M.N., F.M., M.C.C.), Italy.

\*The first 2 authors contributed equally to this work.

The online-only Data Supplement, which contains additional information about Methods, can be found with this article at <http://www.circulationaha.org>.

Correspondence to Antonia Germani, Laboratorio di Patologia Vascolare, Istituto Dermopatico dell'Immacolata-IDI, Via Monti di Creta 104, 00167 Rome, Italy. E-mail [a.germani@idi.it](mailto:a.germani@idi.it)

© 2004 American Heart Association, Inc.

*Circulation* is available at <http://www.circulationaha.org>

DOI: 10.1161/01.CIR.0000147776.50787.74

cells.<sup>11,12</sup> In vascular smooth muscle cells, DGC disruption perturbs vascular functions,<sup>13</sup> leading to ischemic lesions and exacerbating muscle damage. The molecular mechanism implicating dystrophin in vascular dysfunction may involve skeletal muscle–derived nitric oxide (neuronal nitric oxide synthase, nNOS), the enzyme that produces the freely diffusible signaling molecule nitric oxide (NO).<sup>14</sup> In skeletal muscle, NO acts as an antiinflammatory molecule, preventing muscle damage.<sup>15</sup> Moreover, NO regulates blood flow in exercising skeletal muscle by antagonizing  $\alpha$ -adrenergic vasoconstriction.<sup>16</sup> It is conceivable that NO produced by nNOS in skeletal muscle fibers could diffuse to nearby arterioles, resulting in vasodilation and increasing blood flow. The dystrophin complex interacts with nNOS, anchoring this protein to the sarcolemma.<sup>17</sup> In DMD and in several murine models of muscular dystrophy, nNOS protein is mislocalized in the cytoplasm, and its expression is reduced.<sup>17–19</sup> Clinical assessment of vascular control in DMD patients<sup>16</sup> and experimental studies in dystrophin-deficient mice<sup>19</sup> revealed an impairment of skeletal muscle contraction to attenuate  $\alpha$ -adrenergic vasoconstriction. More recently, it has been demonstrated that flow (shear stress)–mediated NO-dependent artery dilation is impaired in *mdx* dystrophin-deficient mice.<sup>12,20</sup> Therefore, it was suggested that dystrophin deficiency, through a sustained vascular constriction and inadequate blood flow supply, causes chronic ischemia and contributes to muscle damage.

After ischemia, many factors regulate the consequent neoangiogenic response. In DMD, cytokines and growth factors produced by both resident and inflammatory cells recruited at sites of muscle degeneration<sup>21</sup> may stimulate angiogenesis; conversely, a lack of NO because of nNOS deficiency may hamper this process. The present study assessed whether blood vessel development in response to an acute ischemic event was affected in dystrophin-deficient mice. To this aim, vascularization was examined in a model of hindlimb ischemia in *mdx* mice. It was found that in *mdx* mice, arteriogenesis in response to ischemia was enhanced. Furthermore, bFGF-stimulated vessel formation in subcutaneously injected Matrigel was increased as well in *mdx* mice, and serum derived from *mdx* mice sustained in vitro endothelial cell–derived tubular structure formation more efficiently than the wild-type (WT) counterpart. Finally, faster skin wound healing was observed in *mdx* mice.

## Methods

### Animal Model of Hindlimb Ischemia

Male C57BL/10SnJ (WT) and *mdx* mice (The Jackson Laboratory, Bar Harbor, Me), 2 months of age and weighing 23 to 25 g, were used for all experiments. Animals were housed at constant room temperature ( $24\pm 1^\circ\text{C}$ ) and humidity ( $60\pm 3\%$ ). Hindlimb ischemia was induced by femoral artery dissection as described previously.<sup>22</sup>

Laser Doppler perfusion imaging (LDPI; Liscia) was used to record serial blood flow measurements for 14 days after surgery as described previously.<sup>22</sup>

All experimental procedures complied with the Guidelines of the Italian National Institutes of Health and with the *Guide for the Care and Use of Laboratory Animals* (Institute of Laboratory Animal Resources, National Academy of Sciences, Bethesda, Md) and were approved by the Institutional Animal Care and Use Committee.

### Histology, Immunohistochemistry, and Morphometric Analysis

Histology, immunohistochemistry, and morphometric analysis were performed as described in the online-only Data Supplement.

### Angiogenesis Assays

In vivo and in vitro angiogenic assays are described in the Data Supplement.

### Animal Wound Model

Wound healing was performed as described in the Data Supplement.

### Hematopoietic Colony Assay

Peripheral blood cells were isolated by Ficoll-Histopaque (Sigma) gradient separation and then cultured in Methocult M3534 (Stem Cells Technologies). Briefly,  $10^5$  cells were plated in triplicate in methylcellulose medium containing interleukin-6, interleukin-3, and stem cell factor. After 14 days, colonies containing granulocytes/macrophages (CFU-GM), granulocytes (CFU-G), macrophages (CFU-M), and endothelial cells (CFU-EC) were counted. To evaluate the expansion of stem cell–derived hematopoietic colonies, we grouped together CFU-GM, CFU-G, and CFU-M colonies as representative of colony-forming activity by clonogenic cells.

### Statistical Analysis

All data are expressed as mean  $\pm$  SEM. A Student 2-tailed *t* test was performed, and a probability value of  $P\leq 0.05$  was considered statistically significant.

## Results

### Angiogenic Response to Hindlimb Ischemia

Ischemia was induced in WT and *mdx* mice. LDPI was used to document changes in hindlimb blood flow at the indicated time points after the induction of ischemia. In both strains, blood flow was drastically reduced immediately after femoral artery dissection, and progressive recovery was detected between day 3 and day 14 (Figure 1). At day 7 after surgery, blood flow in the ischemic limb of *mdx* mice was markedly higher than in WT mice ( $0.67\pm 0.26$  versus  $0.33\pm 0.18$ ;  $P<0.03$ ). A significant difference was still evident at day 14 after surgery ( $0.82\pm 0.2$  versus  $0.56\pm 0.17$ ;  $P<0.03$ ). At day 21, blood flow was similar between WT and *mdx* mice (data not shown). Morphometric analysis was performed on adductor muscle sections from WT and *mdx* mice at day 7 after femoral artery dissection, when blood flow by LDPI exhibited the most significant difference between the 2 groups. Although capillary density was similar in both strains at the indicated time point (Figure 1B), the length density of arterioles 4 to 11  $\mu\text{m}$  in diameter was significantly increased in *mdx* compared with WT mice ( $13.6\pm 8.43$  versus  $7.8\pm 4.6$   $\text{mm}/\text{mm}^3$ ,  $P<0.03$ ) (Figure 1C). In nonischemic hindlimbs, capillary and arteriolar density was similar in both WT and *mdx* mice (Figure 1, B and C).

### Angiogenic Response to bFGF in the Matrigel Assay

To explore the angiogenic response to bFGF, Matrigel supplemented with bFGF was injected subcutaneously into the mid-lower abdominal region of control and *mdx* mice. In this model, host endothelial cells and smooth muscle cells migrate and form a vascular network in the Matrigel implants. The number of blood vessels within the implants was first determined in histological sections by Masson's trichrome staining 8 days after implantation (Figure 2A). Quantitative

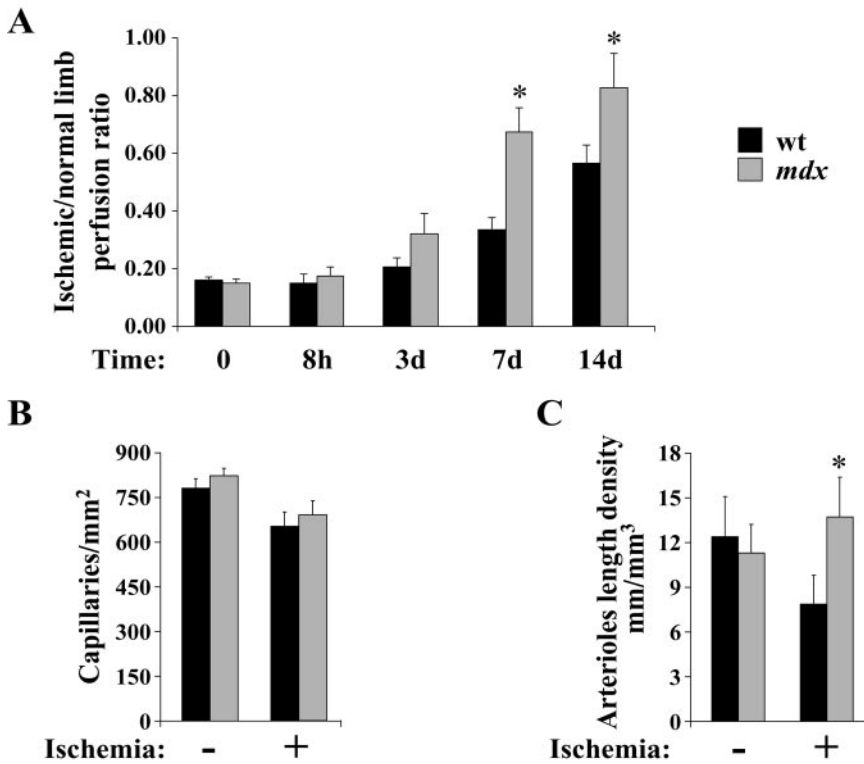


**Figure 1.** Angiogenic response to hind-limb ischemia. A, LDPI was used to quantify both right and left hindlimb perfusion in WT and *mdx* mice immediately after femoral artery dissection (time 0) and at indicated time points after surgery. Graphs show ratio of ischemic to nonischemic perfusion in plantar region of mice. Perfusion ratio before ischemia was 1. At day 7 after surgery, Doppler flow ratio was significantly enhanced in *mdx* mice, and this difference was maintained at day 14 (n=7 per group; \**P*<0.03 vs WT). Capillary (B) and arteriole length density (C) in adductor muscle of control and *mdx* mice at day 7 after femoral artery excision. No difference was detected in capillary density in 2 animal groups. Statistically significant increase in arteriole length density per mm<sup>3</sup> of ischemic tissue was observed in *mdx* vs WT mice (n=6 per group; \**P*<0.03 vs WT).

analysis of the Matrigel plugs revealed that although the absence of bFGF in the Matrigel plugs failed to induce an angiogenic response in both WT and *mdx* mice, the total number of vessels increased in the presence of bFGF in a similar manner in both strains (Figure 2B). However, analysis of histological sections performed by staining vessels with  $\alpha$ -smooth muscle actin antibody, which specifically identifies smooth muscle cells, revealed a significantly higher length density of arterioles (4 to 41  $\mu$ m in diameter) in bFGF-supplemented Matrigel plugs excised from *mdx* mice com-

pared with WT mice (46.9 $\pm$ 14.7 versus 19.5 $\pm$ 5.8 mm/mm<sup>3</sup>) (Figure 2, C and D).

**Angiogenic Response in Wound Repair**

Because neovascularization is a critical component in wound healing and regeneration, we examined whether skin wound closure was accelerated in *mdx* mice. Full-thickness skin wounds were surgically created on the middle back of WT and *mdx* mice. Analysis of wound diameter was performed through digital processing of pictures at the indicated time

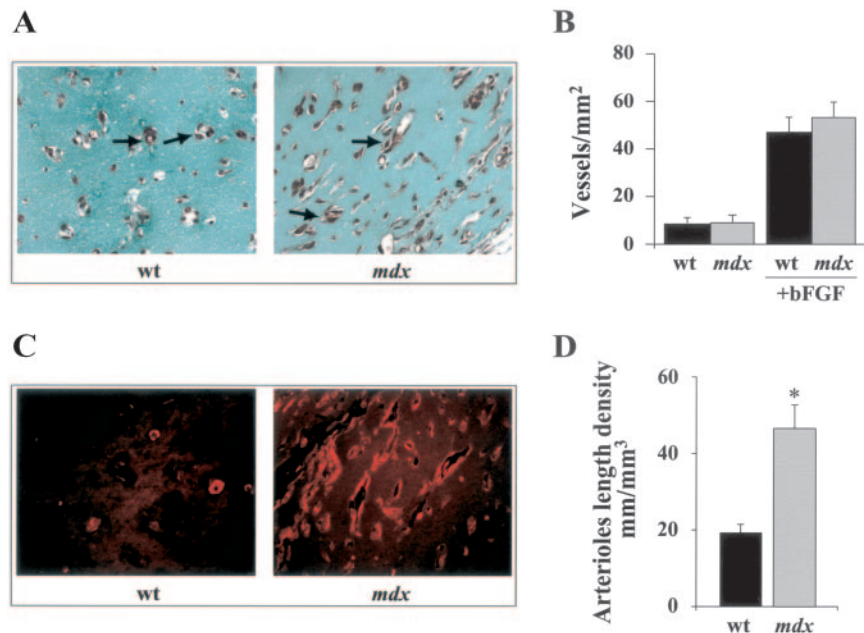


**Figure 2.** Angiogenic response to bFGF in Matrigel plugs. A, Representative photomicrographs of sections from Matrigel plugs supplemented with bFGF, removed from WT and *mdx* mice after 8 days (Masson's trichrome staining; magnification  $\times$ 40). Red blood cells are present in neovessels (arrows). B, Total number of neovessels over whole area of Matrigel was measured and expressed as number of vessels/mm<sup>2</sup>. Note that angiogenesis within Matrigel plugs required bFGF supplementation. No significant differences were detected in number of total vessels between 2 groups of animals. C, Immunohistological analysis of  $\alpha$ -smooth muscle actin expression on Matrigel plug sections from WT and *mdx* mice (magnification  $\times$ 40) staining for  $\alpha$ -actin (in red). D, Quantification of arteriole length density in bFGF-supplemented Matrigel plugs excised from WT and *mdx* mice. *Mdx* mice showed a 50% increase in arteriole length density compared with control mice (n=6 per group; \**P*<0.001).



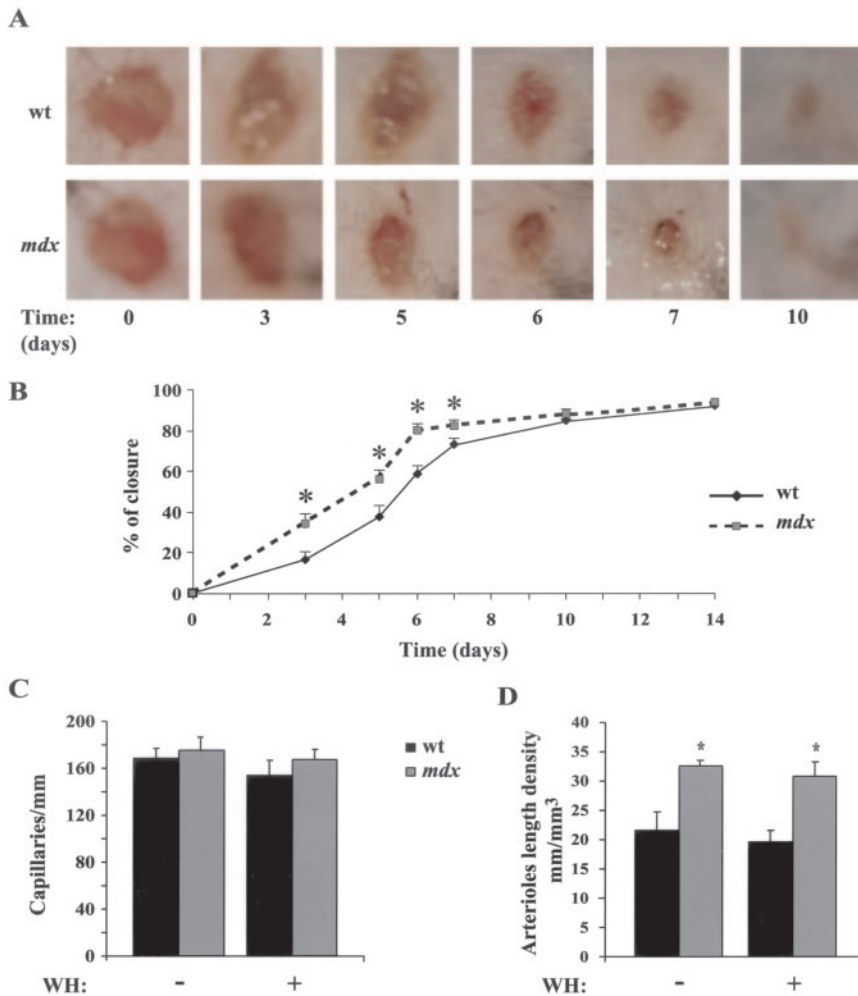


**Figure 3.** Angiogenic response to wound healing. Accelerated healing of full thickness wounds in *mdx* mice compared with WT mice. A, Representative examples show wound healing in *mdx* and WT mice. Wounds were photographed at time indicated from day 0 to 10. Day 0 pictures were taken immediately after wounding. B, Average results showing that wound closure rate was different between WT (wt) and *mdx* mice. Results are presented as percentage of closed wound area vs total area at time 0 after wound. Each time point represents average result from 12 mice. \* $P < 0.02$ .  $P < 0.005$  at day 3, *mdx* vs wild-type. Capillary (C) and arteriole length density (D) in skin of WT and *mdx* mice before (-) and at day 5 (+) of wound healing (WH). No difference was detected in capillary density in 2 animal groups. Statistically significant increase in arteriole length density per  $\text{mm}^3$  was observed in *mdx* vs WT mice, both in normal and in wounded skin ( $n = 4$  per group; \* $P < 0.02$  vs WT).

points (Figure 3A), and the rate of wound healing was expressed as a percentage of closure (Figure 3B). At day 3 after skin injury, areas were reduced by  $34 \pm 15.9\%$  in *mdx* and by  $16.9 \pm 12.6\%$  in WT mice ( $P < 0.005$ ). Statistically significant differences in the percentages of wound closure between the 2 groups persisted at day 5 ( $56 \pm 14.9\%$  versus  $38.8 \pm 9.3\%$ ;  $P < 0.02$ ), day 6 ( $79.4 \pm 10.3\%$  versus  $58.8 \pm 9.3\%$ ,  $P < 0.005$ ), and day 7 ( $82 \pm 9.3\%$  versus  $73 \pm 10.8\%$ ,  $P < 0.02$ ) (Figure 3B). Complete wound closure in both strains was evident by day 14 (Figure 3, A and B). To assess whether the difference in wound healing between WT and *mdx* mice was associated with enhanced skin neovascularization, morphometric analysis was performed on normal skin and on 5-day wounded skin in both WT and *mdx* mice. No difference in capillary density was found between strains before and after wounding (Figure 3C). In contrast, the length density of arterioles 4 to 41  $\mu\text{m}$  in diameter was increased in *mdx* compared with WT mice ( $32.8 \pm 1$  versus  $21.5 \pm 3.4$   $\text{mm}/\text{mm}^3$ ,  $P < 0.02$ ) (Figure 3D), and this difference persisted at day 5 after wounding ( $30.9 \pm 2.7$  versus  $19.6 \pm 2.4$   $\text{mm}/\text{mm}^3$ ,  $P < 0.02$ ) (Figure 3D).

### Serum From *mdx* Mice Accelerates Vascular Structure Formation In Vitro

The following experiments were aimed at determining whether the improved neovascularization in *mdx* mice could

be associated with enhanced release of angiogenic growth factors into the systemic circulation. Human umbilical vein ECs (HUVECs) were plated on Matrigel in the presence of increasing concentrations of serum obtained from either WT or *mdx* mice. In all experimental conditions, HUVECs formed tubular structures, and 90 minutes after plating, branching points were counted to compare the angiogenic potential of serum from WT and *mdx* mice. At the indicated time point, a significant increase in the number of branching points was detected when cells were cultured in the presence of serum obtained from *mdx* mice (Figure 4, A and B). This difference persisted when increasing serum concentrations were used (Figure 4B). To investigate whether the enhanced tubular structure formation was mediated by an increased accumulation of growth factors in serum from *mdx* mice, the concentrations of 4 well-known angiogenic factors, vascular endothelial growth factor, bFGF, stromal-derived factor-1 (SDF-1), and MCP-1, were evaluated by an ELISA method. Although levels of vascular endothelial growth factor, bFGF, and MCP-1 were similar in serum from both strains (data not shown), SDF-1 levels were significantly increased in serum from *mdx* mice ( $1214 \pm 181$  versus  $745 \pm 154$   $\text{pg}/\text{mL}$  in WT mice,  $P < 0.03$ ) (Figure 4C). Blocking antibody to the SDF-1 receptor CXCR4 strongly inhibited tubular structure formation by HUVECs in the presence of 1% of serum from both

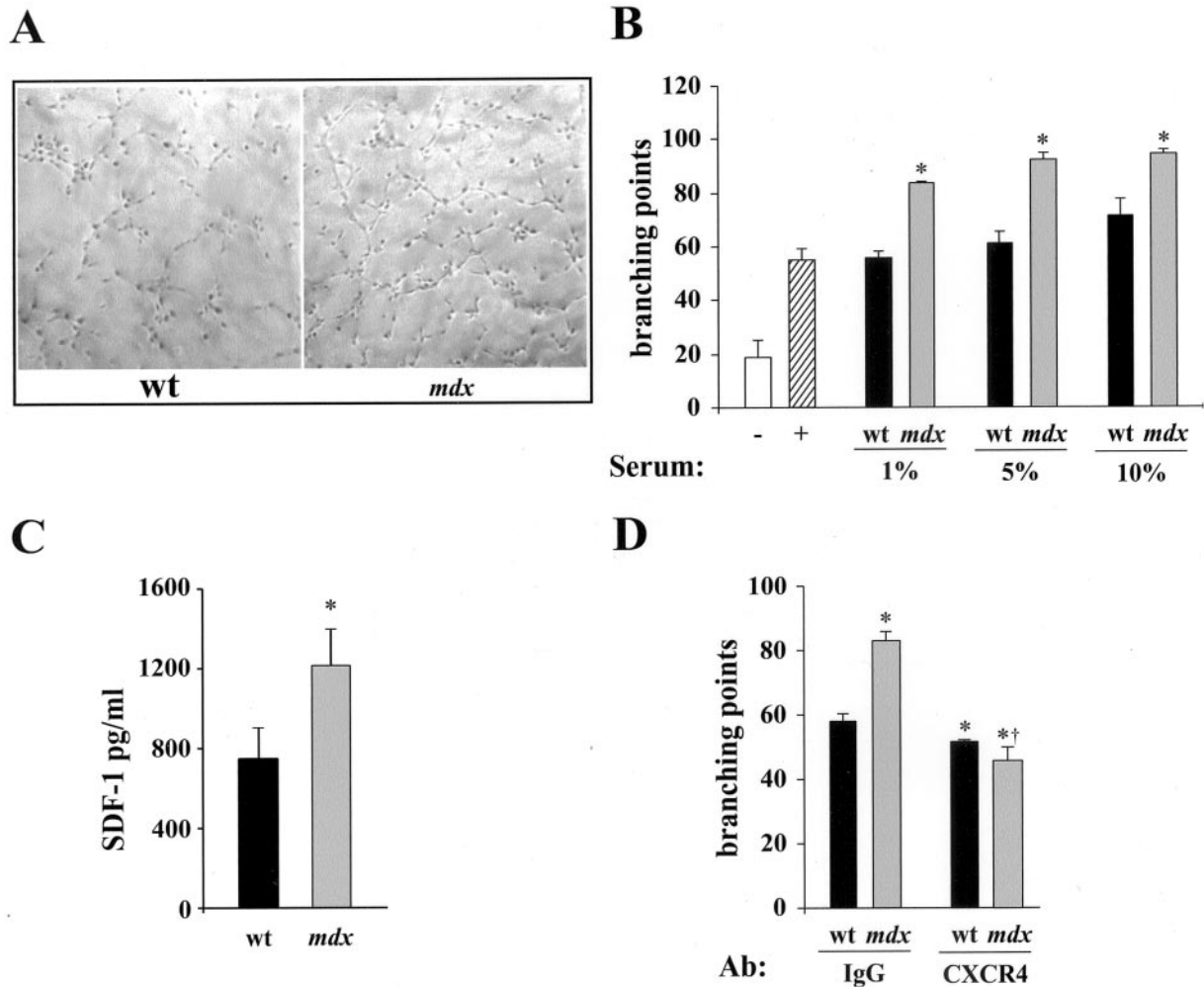


**Figure 4.** Effect of serum from *mdx* mice in in vitro assay of HUVEC differentiation. Serum of *mdx* mice induced organization of HUVECs in tubular structures faster than serum of WT mice. A, Representative photomicrographs of HUVECs plated on Matrigel in EBM2 medium supplemented with 1% serum from WT (left) and *mdx* mice (right). B, Quantification of branching points was performed after 90 minutes in presence of indicated concentrations of serum from WT (*wt*) and *mdx* mice. For negative (-) and positive (+) controls, HUVECs were plated on Matrigel in EBM2 medium either in absence or in presence of growth factors, respectively. Results represent mean of 3 independent experiments performed in duplicate (\* $P < 0.03$ ). C, SDF-1 serum levels in WT and *mdx* mice. In *mdx* mice, amount of SDF-1 was significantly higher than in WT mice (\* $P < 0.03$ ). D, Quantification of branching points obtained by plating HUVECs on Matrigel with blocking antibody to CXCR4 in presence of 1% serum from WT and *mdx* mice. CXCR4 blocking antibody inhibited tubular structure formation, as evaluated by counting branching points as indicated in B (\* $P < 0.03$  and † $P < 0.001$  vs WT and *mdx* IgG-treated, respectively).

WT and *mdx* mice. Under these experimental conditions, *mdx* and WT serum induced the formation of a similar number of branching points (Figure 4D).

**Involvement of Stem Cell Mobilization in Ischemia-Induced Angiogenesis**

Recent experimental results showed that bone marrow-derived stem cells as well as circulating progenitor cells incorporate into foci of damaged tissue, augmenting both skeletal muscle regeneration and neovascularization.<sup>23,24</sup>

In light of these studies, we sought to investigate whether stem cells are involved in the enhanced neovascularization observed in *mdx* mice. To this end, we first analyzed the level of hematopoietic progenitor cells in the peripheral blood of *mdx* mice. By a colony-formation assay using methylcellulose stem cell medium, a 4-fold increase in the number of

circulating hematopoietic progenitors capable of forming CFU colonies (CFU-GM, CFU-G, and CFU-M) was found in the peripheral blood obtained from *mdx* mice compared with WT mice (Figure 5A). Then, we tested the possibility that stem cells contributed to the increased vascularization observed in ischemic muscle of *mdx* mice. Despite the increased number of stem cells in the peripheral blood of *mdx* mice, immunohistological analyses performed to detect stem cells expressing c-kit antigen in hindlimb skeletal muscle tissue did not evidence any significant differences between the 2 strains (data not shown). However, 3 days after ischemia, skeletal muscle from *mdx* mice revealed a 10-fold increase of c-kit-positive (c-kit+) cells compared with those detected in WT mice (Figure 5B). These cells were located close to both the muscle fibers and the vessel walls. Interestingly, some c-kit+ cells associated with vessel walls expressed smooth

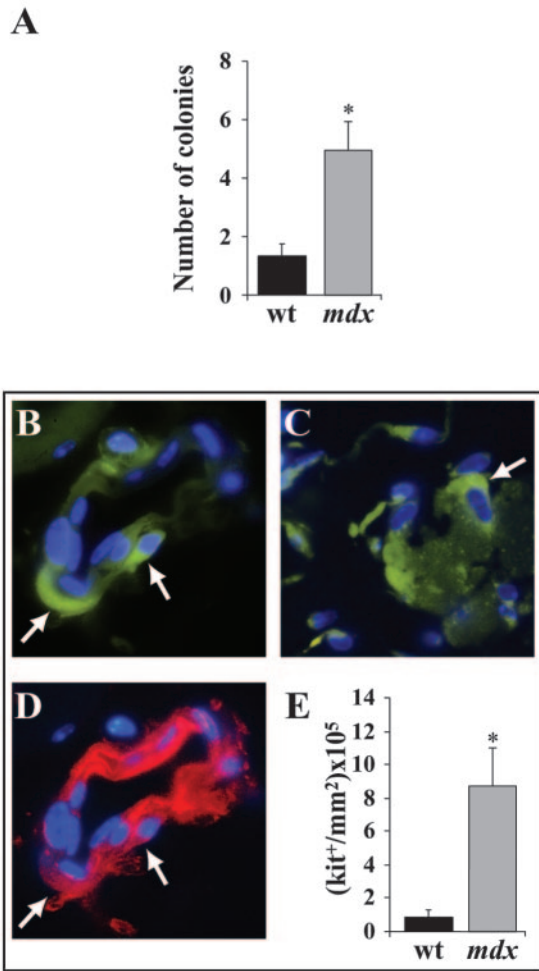


**Figure 5.** Stem cell mobilization and recruitment in *mdx* mice. A, Increased number of circulating hematopoietic stem cells in *mdx* mice. Mononucleated cells recovered from peripheral blood of WT and *mdx* mice were cultured in Methocult M3534. After 14 days, CFU-GM, CFU-G, and CFU-M were counted and expressed as hematopoietic colonies. B, Immunodetection of stem cells c-kit<sup>+</sup> (green fluorescence and arrows) in vessel wall and C, in ischemic skeletal muscle (arrows) from *mdx* mice. D, c-kit<sup>+</sup> cells in same blood vessel wall as shown in B expressed smooth muscle actin (red fluorescence and arrows). E, Number of c-kit<sup>+</sup> cells 3 days after femoral artery excision was markedly higher in *mdx* than in WT muscle. Bar graph of mean c-kit<sup>+</sup> cells expressed as number/mm<sup>2</sup> × 10<sup>3</sup> in WT and *mdx* ischemic skeletal muscle. \**P*<0.05 vs WT.

muscle actin (Figure 5B), indicating their differentiation into smooth muscle cells.

### Discussion

The present study identifies a link between dystrophin and neovascularization. *Mdx* mice, lacking functional dystrophin, showed enhanced vascularization of ischemic hindlimbs, accelerated wound healing, and improved vessel growth in bFGF-infiltrated Matrigel plugs.

In the absence of ischemia, there was no detectable difference in the vascularization of hindlimb muscle between control and *mdx* mice. However, after ischemia, evidence of enhanced perfusion was obtained from blood flow measurements, and at day 7 after surgery, blood flow was 50% higher

in *mdx* limbs than in limbs from control mice. Consistent with this result, ischemic hindlimbs from *mdx* mice presented, at day 7 after surgery, a significant increase in small arteriolar length density, whereas no change in capillary density was detected. Vascularization plays a key role in tissue repair, and skeletal muscle tissues of *mdx* mice show degeneration and regeneration between 2 and 12 weeks of age. Increased vasculogenesis may represent an adaptive response of the organism to pathological levels of muscle regeneration.

The enhanced number of arterioles after ischemia and in the *in vivo* bFGF Matrigel plug assay indicates that *mdx* mouse neovascularization occurs through the activation of an arteriogenic response. In contrast, at least under the experimental conditions of the present study, capillary number was not affected.

Acceleration of the regenerative process is not restricted to skeletal muscle, because wound closure was also improved in *mdx* skin. Indeed, efficient wound repair is a coordinated process that requires not only an increase in the synthesis and deposition of collagen and migration of fibroblasts and keratinocytes into the wound area but also neovascularization. In contrast to skeletal muscle, a significant increase in arteriole length density was found in *mdx* mouse normal skin versus WT mouse skin, and this difference persisted at 5 days after wounding.

To date, we do not know whether enhanced vascularization is a direct consequence of the lack of functional dystrophin. The use of animal models of muscular dystrophy with a functional dystrophin and DGC complex,<sup>10</sup> as well as dystrophin-overexpressing *mdx* mice,<sup>25</sup> could help understand the role of dystrophin in neovascularization. Secondary mechanisms, such as the inflammatory response to muscle damage, could be responsible for increased arteriogenesis and regeneration in *mdx* mice. Conversely, a systemic imbalance of cytokines and growth factors may stimulate regenerative processes and inhibit others, eg, skeletal muscle fiber maturation. It is well accepted that the inflammatory response to myofiber damage is a compelling candidate mechanism for the exacerbation of DMD.<sup>21</sup> Cytokines and chemokines released by DMD muscle may play an important role in recruiting leukocytes and macrophages, which in turn can act as a source of more cytokines and growth factors. Indeed, bFGF,<sup>6</sup> MCP-1,<sup>7,8</sup> nerve growth factor,<sup>9</sup> and PDGF<sup>26</sup> are upregulated in *mdx* mouse skeletal muscle, and some of these factors are also enhanced in the serum of DMD patients. These factors are all potent stimulators of arteriogenesis<sup>27</sup> and can act as chemoattractants for satellite cells and stem cells. Consistent with these findings, we showed that serum obtained from *mdx* mice significantly enhanced HUVEC reorganization in tubular structures on Matrigel. Interestingly, we detected increased levels of the chemokine SDF-1 in *mdx* mouse serum. Blocking antibody to the SDF-1 receptor CXCR4 inhibited tubular structure formation on Matrigel assay, demonstrating that the increased levels of SDF-1 may be responsible for the enhanced vascularization in *mdx* mice.<sup>28,29</sup> It is noteworthy that SDF-1 is essential for mobilization and recruitment of stem cells and smooth muscle progenitor cells into damaged tissues.<sup>30–32</sup> This may explain why enhanced arteriogenesis was evidenced in *mdx* mice.



Indeed, we found an increased number of circulating bone marrow progenitor cells in serum from *mdx* mice. In the absence of ischemia, c-kit<sup>+</sup> cells were rarely detected in skeletal muscle of both WT and *mdx* mice (data not shown). However, after ischemia, the number of stem cells expressing c-kit antigen increased in ischemic hindlimb of *mdx* mice. Interestingly, in *mdx* mice, stem cells were located close to muscle fibers and vessel walls. Thus, in *mdx* mice, stem cell mobilization and recruitment were exacerbated after ischemia, possibly contributing to increased vascularization.

The NOS pathway plays an important role in the regulation of muscle and endothelial cell proliferation, survival, and differentiation.<sup>33</sup> Our results suggest that NO does not influence vascularization in the absence of functional dystrophin. In *mdx* mice, decreased levels of NO exacerbate inflammation and muscular injury. Normalization of NO production attenuated skeletal muscle damage and inflammation without affecting angiogenesis.<sup>34</sup> Recently, Loufrani et al<sup>35</sup> demonstrated that endothelium-dependent vascular smooth muscle relaxation was altered in *mdx* mice, resulting in attenuation of flow-induced vasodilation. Moreover, the same authors showed that vessel density was decreased in gracilis muscle of *mdx* mice. This result is apparently in contrast with our results showing the lack of differences in capillary and arteriolar length density between the adductor muscle from *mdx* and control mice. Indeed, different contributions of fast and slow fibers in skeletal muscle composition may explain this discrepancy. In rodents, nNOS is specifically expressed in fast- but not in slow-twitch muscle,<sup>36</sup> and unlike the adductor muscle examined in our study, gracilis is a fast-twitch muscle. Thus, the diminished arteriolar density in gracilis muscle of *mdx* mice may represent the result of a local decrease of NO bioavailability that may not be present throughout the organism. Furthermore, in the present study, arteriole and capillary densities were evaluated in 2-month-old animals, ie, when maximal skeletal muscle degeneration and regeneration are expected to occur.<sup>37</sup> In contrast, Loufrani et al used 3.5-month-old *mdx* mice in which only small patches of necrosis and regeneration were seen. This suggests that the active inflammatory response in the acute phase of ongoing muscle degeneration may play a role in the enhanced arteriogenic response observed under the experimental conditions of our study. Thus, enhanced arteriogenesis may be attenuated at earlier or later periods when the pathological manifestations are less severe.

In conclusion, we propose that DMD is characterized by an imbalance of cytokine and growth factors; this imbalance may play an important role in DMD pathogenesis, disrupting normal neovascularization and enhancing recruitment of inflammatory cells.

### Acknowledgments

This work was supported by grants from Telethon (GGP02284) and the Italian Ministry of Health. We thank Dr Francesco Facchiano for technical support and helpful suggestions. We also thank Maurizio Inzillo and the Medical Imaging Service of Istituto Dermatologico dell'Immacolata for figure preparation.

### References

- Cohn RD, Campbell KP. Molecular basis of muscular dystrophies. *Muscle Nerve*. 2000;23:1456–1471.
- Spence HJ, Chen YJ, Winder SJ. Muscular dystrophies, the cytoskeleton and cell adhesion. *Bioessays*. 2002;24:542–552.
- Henry MD, Campbell KP. A role for dystroglycan in basement membrane assembly. *Cell*. 1998;95:859–870.
- Emery AE. The muscular dystrophies. *Lancet*. 2002;359:687–695.
- Sicinski P, Geng Y, Ryder-Cook AS, Barnard EA, Darlison MG, Barnard PJ. The molecular basis of muscular dystrophy in the *mdx* mouse: a point mutation. *Science*. 1989;244:1578–1580.
- D'Amore PA, Brown RH Jr, Ku PT, Hoffman EP, Watanabe H, Arahata K, Ishihara T, Folkman J. Elevated basic fibroblast growth factor in the serum of patients with Duchenne muscular dystrophy. *Ann Neurol*. 1994;35:362–365.
- Fang J, Shi GP, Vaghy PL. Identification of the increased expression of monocyte chemoattractant protein-1, cathepsin S, UPIX-1, and other genes in dystrophin-deficient mouse muscles by suppression subtractive hybridization. *J Cell Biochem*. 2000;79:164–172.
- Porter JD, Guo W, Merriam AP, Khanna S, Cheng G, Zhou X, Andrade FH, Richmonds C, Kaminski HJ. Persistent over-expression of specific CC class chemokines correlates with macrophage and T-cell recruitment in *mdx* skeletal muscle. *Neuromuscul Disord*. 2003;13:223–235.
- Toti P, Villanova M, Vatti R, Schuerfeld K, Stumpo M, Barbagli L, Malandrini A, Costantini M. Nerve growth factor expression in human dystrophic muscles. *Muscle Nerve*. 2003;27:370–373.
- Bansal D, Miyake K, Vogel SS, Groh S, Chen CC, Williamson R, McNeil PL, Campbell KP. Defective membrane repair in dysferlin-deficient muscular dystrophy. *Nature*. 2003;423:168–172.
- Harricane MC, Fabbrizio E, Lees D, Prades C, Travo P, Mornet D. Dystrophin does not influence regular cytoskeletal architecture but is required for contractile performance in smooth muscle aortic cells. *Cell Biol Int*. 1994;18:947–958.
- Loufrani L, Matrougui K, Gorny D, Duriez M, Blanc I, Levy BI, Henrion D. Flow (shear stress)-induced endothelium-dependent dilation is altered in mice lacking the gene encoding for dystrophin. *Circulation*. 2001;103:864–870.
- Coral-Vazquez R, Cohn RD, Moore SA, Hill JA, Weiss RM, Davisson RL, Straub V, Barresi R, Bansal D, Hrstka RF, Williamson R, Campbell KP. Disruption of the sarcoglycan-sarcospan complex in vascular smooth muscle: a novel mechanism for cardiomyopathy and muscular dystrophy. *Cell*. 1999;98:465–474.
- Michel T, Feron O. Nitric oxide synthases: which, where, how, and why? *J Clin Invest*. 1997;100:2146–2152.
- Nguyen HX, Tidball JG. Expression of a muscle-specific, nitric oxide synthase transgene prevents muscle membrane injury and reduces muscle inflammation during modified muscle use in mice. *J Physiol*. 2003;550:347–356.
- Sander M, Chavoshan B, Harris SA, Iannaccone ST, Stull JT, Thomas GD, Victor RG. Functional muscle ischemia in neuronal nitric oxide synthase-deficient skeletal muscle of children with Duchenne muscular dystrophy. *Proc Natl Acad Sci U S A*. 2000;97:13818–13823.
- Brennan JE, Chao DS, Xia H, Aldape K, Bredt DS. Nitric oxide synthase complexed with dystrophin and absent from skeletal muscle sarcolemma in Duchenne muscular dystrophy. *Cell*. 1995;82:743–752.
- Chang WJ, Iannaccone ST, Lau KS, Masters BS, McCabe TJ, McMillan K, Padre RC, Spencer MJ, Tidball JG, Stull JT. Neuronal nitric oxide synthase and dystrophin-deficient muscular dystrophy. *Proc Natl Acad Sci U S A*. 1996;93:9142–9147.
- Thomas GD, Shaul PW, Yuhanna IS, Froehner SC, Adams ME. Vasomodulation by skeletal muscle-derived nitric oxide requires  $\alpha$ -syntrophin-mediated sarcolemmal localization of neuronal nitric oxide synthase. *Circ Res*. 2003;92:554–560.
- Loufrani L, Levy BI, Henrion D. Defect in microvascular adaptation to chronic changes in blood flow in mice lacking the gene encoding for dystrophin. *Circ Res*. 2002;91:1183–1189.
- Porter JD, Khanna S, Kaminski HJ, Rao JS, Merriam AP, Richmonds CR, Leahy P, Li J, Guo W, Andrade FH. A chronic inflammatory response dominates the skeletal muscle molecular signature in dystrophin-deficient *mdx* mice. *Hum Mol Genet*. 2002;11:263–272.
- Germani A, Di Carlo A, Mangoni A, Straino S, Giacinti C, Turrini P, Biglioli P, Capogrossi MC. Vascular endothelial growth factor modulates skeletal myoblast function. *Am J Pathol*. 2003;163:1417–1428.
- Rafii S, Lyden D. Therapeutic stem and progenitor cell transplantation for organ vascularization and regeneration. *Nat Med*. 2003;9:702–712.
- Charge SB, Rudnicki MA. Cellular and molecular regulation of muscle regeneration. *Physiol Rev*. 2004;84:209–238.

25. Scott JM, Li S, Harper SQ, Welikson R, Bourque D, DelloRusso C, Hauschka SD, Chamberlain JS. Viral vectors for gene transfer of micro-, mini-, or full-length dystrophin. *Neuromuscul Disord.* 2002;12(suppl 1):S23–S29.
26. Zhao Y, Haginoya K, Sun G, Dai H, Onuma A, Inuma K. Platelet-derived growth factor and its receptors are related to the progression of human muscular dystrophy: an immunohistochemical study. *J Pathol.* 2003;201:149–159.
27. Carmeliet P. Mechanisms of angiogenesis and arteriogenesis. *Nat Med.* 2000;6:389–395.
28. Salcedo R, Wasserman K, Young HA, Grimm MC, Howard OM, Anver MR, Kleinman HK, Murphy WJ, Oppenheim JJ. Vascular endothelial growth factor and basic fibroblast growth factor induce expression of CXCR4 on human endothelial cells: in vivo neovascularization induced by stromal-derived factor-1 $\alpha$ . *Am J Pathol.* 1999;154:1125–1135.
29. Salvucci O, Yao L, Villalba S, Sajewicz A, Pittaluga S, Tosato G. Regulation of endothelial cell branching morphogenesis by endogenous chemokine stromal-derived factor-1. *Blood.* 2002;99:2703–2711.
30. Petit I, Szyper-Kravitz M, Nagler A, Lahav M, Peled A, Habler L, Ponomaryov T, Taichman RS, Arenzana-Seisdedos F, Fujii N, Sandbank J, Zipori D, Lapidot T. G-CSF induces stem cell mobilization by decreasing bone marrow SDF-1 and up-regulating CXCR4. *Nat Immunol.* 2002;3:687–694.
31. Askari AT, Unzek S, Popovic ZB, Goldman CK, Forudi F, Kiedrowski M, Rovner A, Ellis SG, Thomas JD, DiCorleto PE, Topol EJ, Penn MS. Effect of stromal-cell-derived factor 1 on stem-cell homing and tissue regeneration in ischaemic cardiomyopathy. *Lancet.* 2003;362:697–703.
32. Schober A, Knarren S, Lietz M, Lin EA, Weber C. Crucial role of stromal cell-derived factor-1 $\alpha$  in neointima formation after vascular injury in apolipoprotein E-deficient mice. *Circulation.* 2003;108:2491–2497.
33. Anderson JE. A role for nitric oxide in muscle repair: nitric oxide-mediated activation of muscle satellite cells. *Mol Biol Cell.* 2000;11:1859–1874.
34. Wehling M, Spencer MJ, Tidball JG. A nitric oxide synthase transgene ameliorates muscular dystrophy in mdx mice. *J Cell Biol.* 2001;155:123–131.
35. Loufrani L, Dubroca C, You D, Li Z, Levy B, Paulin D, Henrion D. Absence of dystrophin in mice reduces NO-dependent vascular function and vascular density: total recovery after a treatment with the aminoglycoside gentamicin. *Arterioscler Thromb Vasc Biol.* 2004;24:671–676.
36. Stamler JS, Meissner G. Physiology of nitric oxide in skeletal muscle. *Physiol Rev.* 2001;81:209–237.
37. Grady RM, Teng H, Nichol MC, Cunningham JC, Wilkinson RS, Sanes JR. Skeletal and cardiac myopathies in mice lacking utrophin and dystrophin: a model for Duchenne muscular dystrophy. *Cell.* 1997;90:729–738.



**Enhanced Arteriogenesis and Wound Repair in Dystrophin-Deficient *mdx* Mice**  
Stefania Straino, Antonia Germani, Anna Di Carlo, Daniele Porcelli, Roberta De Mori,  
Antonella Mangoni, Monica Napolitano, Fabio Martelli, Paolo Biglioli and Maurizio C.  
Capogrossi

*Circulation*. 2004;110:3341-3348; originally published online November 15, 2004;  
doi: 10.1161/01.CIR.0000147776.50787.74

*Circulation* is published by the American Heart Association, 7272 Greenville Avenue, Dallas, TX 75231  
Copyright © 2004 American Heart Association, Inc. All rights reserved.  
Print ISSN: 0009-7322. Online ISSN: 1524-4539

The online version of this article, along with updated information and services, is located on the  
World Wide Web at:

<http://circ.ahajournals.org/content/110/21/3341>

Data Supplement (unedited) at:

<http://circ.ahajournals.org/content/suppl/2004/11/22/01.CIR.0000147776.50787.74.DC1>

**Permissions:** Requests for permissions to reproduce figures, tables, or portions of articles originally published in *Circulation* can be obtained via RightsLink, a service of the Copyright Clearance Center, not the Editorial Office. Once the online version of the published article for which permission is being requested is located, click Request Permissions in the middle column of the Web page under Services. Further information about this process is available in the [Permissions and Rights Question and Answer](#) document.

**Reprints:** Information about reprints can be found online at:  
<http://www.lww.com/reprints>

**Subscriptions:** Information about subscribing to *Circulation* is online at:  
<http://circ.ahajournals.org/subscriptions/>